

# Probabilistic estimation of seismic economic losses of portal-like precast industrial buildings

Cristoforo Demartino<sup>\*1,3</sup>, Ivo Vanzi<sup>2a</sup> and Giorgio Monti<sup>1,3b</sup>

<sup>1</sup>College of Civil Engineering, Nanjing Tech University, Nanjing 211816, PR China

<sup>2</sup>Department of Engineering and Geology, University "G. d'Annunzio" of Chieti-Pescara, viale Pindaro, Pescara, Italy

<sup>3</sup>DISG, Sapienza University of Rome, via A. Gramsci 53, 00197 Rome, Italy

(Received September 5, 2016, Revised June 2, 2017, Accepted November 22, 2017)

**Abstract.** A simplified framework for the probabilistic estimation of economic losses induced by the structural vulnerability in single-story and single-bay precast industrial buildings is presented. The simplifications introduced in the framework are oriented to the definition of an expeditious procedure adoptable by government agencies and insurance companies for preliminary risk assessment. The economic losses are evaluated considering seismic hazard, structural response, damage resulting from the structural vulnerability and only structural-vulnerability-induced economic losses, i.e., structural repair or reconstruction costs (stock and flow costs) and content losses induced by structural collapse. The uncertainties associated with each step are accounted for via Monte Carlo simulations. The estimation results in a probabilistic description of the seismic risk of portal-like industrial buildings, expressed in terms of economic losses for each occurrence (i.e., seismic event) that owners (i.e., insured) and stakeholders can use to make risk management decisions. The outcome may also be useful for the definition of the insurance premiums and the evaluation of the risks and costs for the owner corresponding to the insurance industrial costs. A prototype of a precast concrete industrial building located in Mirandola, Italy, hit by the 2012 Emilia earthquake, is used as an example of the application of the procedure.

**Keywords:** structural vulnerability; insurance policy; uncertainties; monte carlo

## 1. Introduction

Industry is the organized production of economic goods or services within an economy, and can be carried out while profits outweigh costs. Costs include production factors (labor, capital, or land), taxation and risk. Risk is the possibility of loss resulting from a given action, activity and/or inaction, foreseen or unforeseen. It may be defined as the probability that exposure to a hazard will lead to a negative consequence.

Over recent years, the economic impacts of natural hazards and disasters received much attention. The reliable estimation of the economic, as well as human, losses incurred by an earthquake is a need for the development of seismic risk scenarios, which are now widely accepted as an essential tool for seismic risk management. In particular, the economic impacts deriving by earthquakes received significant interest in the research community. Devastating earthquakes in China (2008 and 2010), New Zealand (2011), Japan (2011) and Italy (2009, 2012 and 2016-17) have tightened the social and the political focus on the

seismic risk emanating from industrial facilities.

The Italian Emilia-Romagna earthquakes, occurred on May 20th and 29th 2012 (main-events), were classified the costliest events outside of the U.S. in 2012 (Aon Benfield 2013). Italy's state-financing body Cassa Depositi e Prestiti allocated a combined 12 billions of Euros to help in the rebuilding process (Benfield 2013). Insured losses were estimated at approximately 1.5 billion of Euros. The area hit by the earthquake is highly industrialized since the late sixties. Braga *et al.* (2014) reported that Emilia-Romagna (6% of the Italian territory) hosts about 12% of the Italian industrial buildings, one-third of them being warehouses; the most frequent typology is reinforced concrete (85% of the total), more than two-thirds of the precast type. The typical structure used in those areas as industrial building is single storey frame composed of precast concrete elements (Dassori *et al.* 2001). The structure is usually made with slender cantilevering columns and simply supported beams. The foundation is usually built with precast concrete plinths using a precast pocketed base system. The connection between beam and columns is typically assigned to connectors of frictional type. This type of structure showed all its weaknesses during the seismic events (e.g., ReLUIS *et al.* 2012, Parisi *et al.* 2012, Marzo *et al.* 2012, Savoia *et al.* 2012, Liberatore *et al.* 2013, Bournas *et al.* 2014, Magliulo *et al.* 2014, Casotto *et al.* 2015, Ercolino *et al.* 2016, Babič *et al.* 2016, Demartino *et al.* 2017a, b).

Seismic risk can be synthetically described as the probability of loss at a given site and is obtained through the convolution of three parameters: exposure, vulnerability

\*Corresponding author, Ph.D.

E-mail: [cristoforo.demartino@me.com](mailto:cristoforo.demartino@me.com)

<sup>a</sup>Professor

E-mail: [i.vanzi@unich.it](mailto:i.vanzi@unich.it)

<sup>b</sup>Professor

E-mail: [giorgio.monti@uniroma1.it](mailto:giorgio.monti@uniroma1.it)

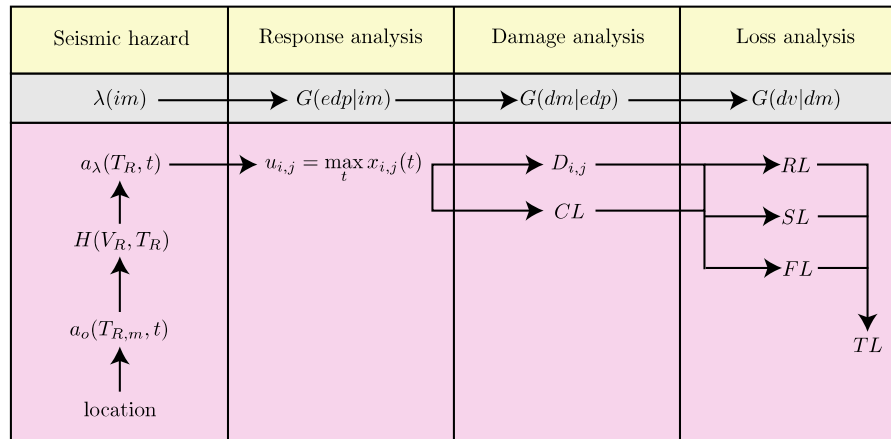


Fig. 1 Performance assessment framework proposed by PEER (Miranda and Aslani 2003) in grey and proposed structural-vulnerability-induced economic losses framework in light red. ( $im$  is the intensity measure of the seismic action,  $\lambda(im)$  is the mean annual frequency of exceedance of  $im$ ,  $edp$  is the engineering demand parameter,  $dm$  is the damage measure and  $dv$  is the loss ratio,  $G(x|y)$  is the conditional probability  $G(X \geq x|Y = y)$ , location is the site coordinates,  $T_R$  is the recurrence interval,  $V_R$  is the exposure period,  $a_0(T_{R,m}, t)$  is the unscaled ground motion time history being  $T_{R,m}$  the different return periods reported by Italian Building Code (NTC-2008 2008),  $H(V_R, T_R)$  is the probability of occurrence of one or more earthquakes within the time period,  $V_R$ , for a Poisson process with return interval,  $T_R$ ,  $a_\lambda(T_R, t)$  is the scaled ground motion time history,  $x_{i,j}(t)$  and  $u_{i,j}$  are the displacement and the maximum displacement of element  $i$  of the portal on its  $j$  (left or right) side,  $D_{i,j}$  is the damage function of the element  $i$  of the portal on its  $j$  (left or right) side,  $CL$  is the collapse function,  $RL$  are the repair losses,  $SL$  are the stock losses,  $FL$  are the flow losses and  $TL$  are the total losses)

and seismic hazard. A fourth parameter may then be added through which the seismic risk can be related to a social or economic loss. Most of the research on the seismic economic loss assessment has led to the development of a general methodology that is usually named PEER framework (Miranda *et al.* 2003). It represents current practice for seismic loss assessment of individual structures and a reference for modern large-scale loss assessment procedures although it has received some criticism (e.g., Der Kiureghian 2005). The methodology can be summarized into four steps: quantification of the seismic hazard, response analysis, definition of the performance groups and damage states and finally loss analysis (Fig. 1). In the same framework, Yang *et al.* (2009) presented a procedure for the seismic performance evaluation of facilities. Moreover, the PEER performance assessment methodology was later adopted by the ATC-58 (2012), using a Monte Carlo simulation procedure to estimate the economic losses.

However, although many approaches for the seismic loss assessment were presented during the last years, little attention has been paid to the specific case of one-story single-bay precast concrete industrial buildings. In particular, the definition of simplified and expeditious procedures for the evaluation of seismic losses using input data easily available by practitioners, by government agencies and by insurance companies seems to be little explored.

This paper presents a simplified framework for the expeditious probabilistic estimation of economic losses induced by structural vulnerability in single-story and single-bay precast industrial buildings. The basic idea of the framework is to provide a tool for expeditious assessment that requires easily available input data consistent with

common building design, construction, and analysis practices. More importantly, this framework has been conceived to be used for regional-scale assessment policies (herein regional scale is understood as territorial study or territorial-related typological study); in fact, such policies can make use of readily available data of structural geometrical characteristics (e.g., from rapid exterior survey and/or existing structural drawings), while information on nonstructural elements and on nature and internal arrangement of the contents, which are continuously changing over time depending on the owners' will, can be acquired only on a case-by-case basis. For these reasons, the focus of the present study is on the economic losses induced by the structural vulnerability. The framework is presented in Section 2. A prototype of a single bay precast concrete industrial building located in Mirandola, Italy, hit by the Emilia earthquake of 2012, is used as an example to illustrate the economic loss assessment procedure (Section 3). Finally, the results are used for the probabilistic evaluation of risks of the insurance policy terms for both insured and insurance companies.

## 2. Framework for the economic loss estimation

A framework for the probabilistic estimation of economic losses induced by the structural vulnerability in single-story and single-bay precast industrial buildings (Fig. 1), based on Matlab, is presented in this Section.

### 2.1 Seismic input and hazard

Following the approach proposed in the Italian Building Code (NTC-2008 2008), given the location, nine groups of

accelerograms corresponding to different return periods ( $T_{R,m}=30, 50, 72, 101, 140, 201, 475, 975, 2475$  years) are first selected. Each group contains 7 independent time histories; each time history is independent in terms of horizontal and vertical components ( $a_{o,h}(T_{R,m},t)$  and  $a_{o,v}(T_{R,m},t)$ ). The ground-motion time histories are simulated using SIMQKE (SIMulation of earthQuaKE ground motions). This software generates groups of stationary artificial ground-motion time histories so as to fit (in an average sense) the target spectrum (Vanmarcke *et al.* 1976). The target spectra are selected according to the Italian Building Code (NTC-2008 2008) starting from the location. The variation of the frequency content (i.e., different shape of the elastic spectra) is accounted only for the horizontal component by the Italian Building Code (NTC-2008 2008) by varying the elastic response spectra shape for different return intervals. Differently, the vertical component has the same elastic response spectra shape for all the return periods. The total duration of the ground-motion time histories is set equal 25 s and the duration of the pseudo-stationary part is set equal to 10 s according to the Italian Building Code (NTC-2008 2008).

In order to evaluate ground-motion time histories with return interval,  $T_R$ , within the nine values of  $T_{R,m}$  given by the Italian Building Code (NTC-2008 2008), a simple transformation is introduced by uniformly scaling up or down the amplitudes

$$a_\lambda(t) = \lambda a_0(t) \quad (1)$$

where  $a_0(t)$  is the unscaled ground motion time history,  $a_\lambda(t)$  is the scaled ground motion time history and  $t$  is the time. A value of  $\lambda=1$  means the natural unscaled ground motion time history is used,  $\lambda<1$  is a scaled-down ground motion time history, while  $\lambda>1$  corresponds to a scaled-up one. This procedure is a combination of the Incremental Dynamic Analysis (IDA) (Vamvatsikos *et al.* 2002, Colapietro *et al.* 2014) and to the Multiple Stripe Analysis (MSA) (Jalayer 2003). In fact, IDA adopts a single set of ground motions scaled to different intensity levels while MSA adopts a different set of ground motions at each intensity level.

The value of  $\lambda$  is estimated using the peak ground acceleration,  $a_g$ , in the interpolation from the data provided (equation according to the Italian Building Code (NTC-2008 2008))

$$\log(a_g(T_R)) = \log(a_g(T_{R,1})) + \log\left(\frac{a_g(T_{R,2})}{a_g(T_{R,1})}\right) \cdot \log\left(\frac{T_R}{T_{R,1}}\right) \cdot \left(\log\left(\frac{T_{R,2}}{T_{R,1}}\right)\right)^{-1} \quad (2)$$

where  $T_{R,1}$  and  $T_{R,2}$  are the return intervals  $T_{(R,m)}$  closer to  $T_R$  reported in the Italian Building Code. Combining Eq. (1) and Eq. (2) the value of  $\lambda$  is found

$$\lambda(T_R) = \frac{a_\lambda(T_R, t)}{a_0(T_R, t)} = \frac{10^{\log(a_g(T_R))}}{a_0(T_{R,1})} \quad (3)$$

Combining the variation of the frequency content (i.e., different groups of ground motion time-histories) and

amplitude with  $T_R$  (i.e., Eq. (3)), the scaled ground-motion time histories are given by

$$a_\lambda(t) = \begin{cases} 1 \cdot a_0(30, t) & T_R < 30 \text{ years} \\ \lambda \cdot a_0(30, t) & 30 < T_R < 50 \text{ years} \\ \vdots & \vdots \\ \lambda \cdot a_0(975, t) & 975 < T_R < 2475 \text{ years} \\ 1 \cdot a_0(2475, t) & \text{if } T_R > 2475 \text{ years} \end{cases} \quad (4)$$

Using this procedure, the ground time histories are scaled in each group across all frequencies while keeping frequency content intact therefore accounting for the variation of the frequency content for different return intervals.

In order to estimate the seismic hazard, an earthquake time recurrence model has to be assumed (Anagnos *et al.* 1988). A traditional choice is the Poisson model (Cornell 1968) that considers earthquakes as independent and stationary events. Accordingly, the probability of occurrence of one or more earthquakes within the exposure period,  $V_R$ , for a Poisson process with return interval,  $T_R$ , is expressed as follows

$$H(n \geq 1, V_R, T_R) = 1 - \exp\left(-\frac{V_R}{T_R}\right) \quad (5)$$

where  $n$  is the number of events within  $V_R$ . Accordingly, once the exposure period is assigned, the hazard function is defined as an exponential distribution.

In this framework,  $V_R$  is the time window in which the economic losses are estimated. Subsequently, once  $V_R$  is assigned, inputs values of  $T_R$  are randomly generated according to the probability distribution in Eq. (5); this will be described in Section 2.5. Using this procedure, independent earthquakes were selected according to the probability of occurrence at the studied location; however, all information concerning the actual time sequence of seismic events within  $V_R$ , is lost. In this way, the possibility of summation of damages generated by more than one earthquake (also neglecting foreshocks, mainshocks and aftershocks) within  $V_R$  is not taken into account. Accordingly, this framework evaluates structural-vulnerability-induced economic losses for each occurrence (i.e., seismic event) starting from undamaged conditions.

It is important to notice that the choice of artificial accelerograms used to compute the statistics of the economic losses, stems from at least three different considerations: (i) the difficulty of selecting groups of natural accelerograms having 3 components for each return period, (ii) easy extendibility of the procedure to different areas characterized by different spectra, and more importantly (iii) the search for consistency of the economic loss statistics with the structural code methodologies. Any alternative definition of the seismic input would not fall within the scope of this study.

## 2.2 Nonlinear dynamic model of the transverse response of a precast frame

One-story industrial buildings are characterized by long-span roof beams, which provide the large open areas needed for manufacturing (Dassori *et al.* 2001, Bonfanti *et al.*

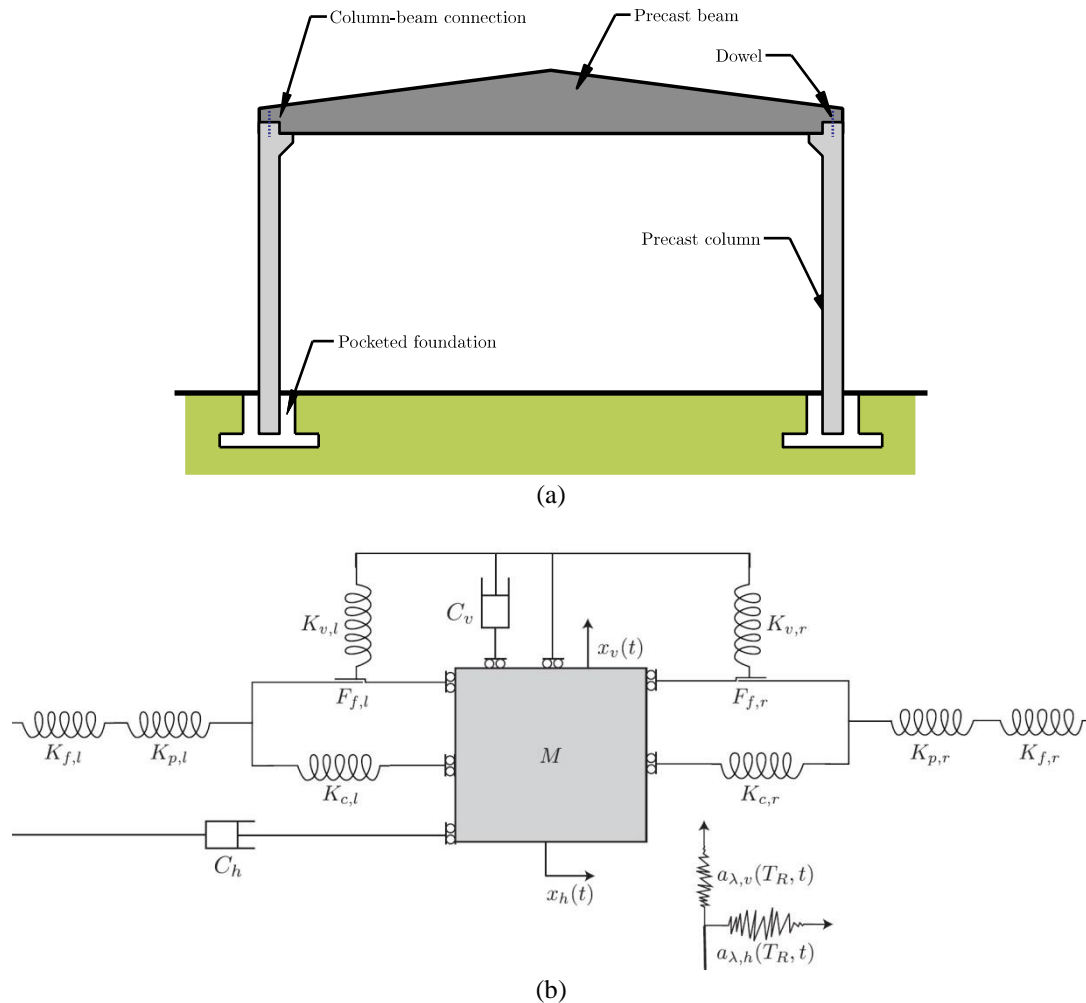


Fig. 2 (a) Typical structure of one-story single-bay precast concrete industrial building, (b) Mechanical model of one-story single-bay precast concrete industrial building

2008). The buildings are usually rectangular. Transverse bay widths usually range from 10 to 25 m, and longitudinal bay widths range from 6 to 8 m. Story heights also range from 6 and 8 m. These buildings are made of precast frames. Each precast frame is composed of two foundation systems, two columns and one beam (Fig. 2(a)).

Foundation systems are usually realized using precast socket footings often not designed to carry the horizontal forces originating from the seismic loads. Vertical loads are transmitted to the foundation by skin friction and end bearing forces. The columns and beams are made of precast concrete elements. In non-seismic designed structures, beam-to-column connections shear transfer is based on friction (concrete-to-concrete or rubber-to-concrete surfaces) and a dowel is often added with the aim of centering column and beam.

The mechanical model of the precast industrial buildings should faithfully reproduce the complete 3D behavior. In fact, damages to these buildings occurred due to a number of additional causes such as failure of the connections between roof elements and supporting beams and to overturning of the lateral infill elements (e.g., ReLUIS *et al.* 2012, Parisi *et al.* 2012, Marzo *et al.* 2012, Savoia *et al.* 2012, Liberatore *et al.* 2013, Bournas *et al.* 2014, Magliulo

*et al.* 2014, Ercolino *et al.* 2016). The seismic performance of industrial precast concrete buildings modeling the complete 3D behavior (i.e., the entire structure) was investigated in many studies (Magliulo *et al.* 2008, Casotto *et al.* 2015, Ercolino *et al.* 2016, Babič *et al.* 2016). On the other hand, many authors proposed a simplified 2D model capable to reproduce the transverse response of one frame of a precast concrete industrial building (i.e., portal-like model) modeling with different level of complexity the non-linear behavior of the foundations, of the columns and of the beam-to-column connections (Liberatore *et al.* 2013, Magliulo *et al.* 2014, Casotto *et al.* 2015, Asprone *et al.* 2016, Demartino *et al.* 2017). These simplified approaches are based on the evidence of the Emilia Romagna earthquakes in which the main damages were observed in (i) the foundations with the presence of inelastic rotations with final non-verticality of the columns, in (ii) the base of the columns with formation of plastic hinges experiencing inelastic rotations and in (iii) the beam-to-column connections with large sliding experiencing large relative displacements (ReLUIS *et al.* 2012). With the aim of deriving a simplified approach for expeditious probabilistic estimation of structural-vulnerability-induced economic losses, a portal-like model will be adopted in the following.

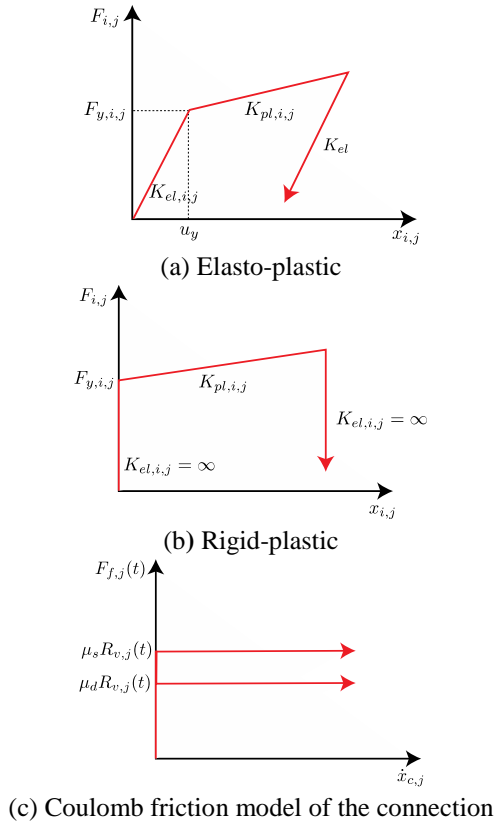


Fig. 3 Force-displacement relationships

The simplified 2D model is a statically determined structure modeled as a two Degree of Freedom oscillators, as represented in Fig. 2(b). This model neglects the presence of the column mass because generally much lower than the mass of the beam and of the roof system and considers only the beam and the roof system masses. The mass of the whole system is considered lumped at the midspan of the beam and the column and beam cross-sections are considered constant with equivalent characteristics to the real one. The axial deformability of the columns and of the beam is neglected. The beam is modeled as a simply supported element with elastic behavior. The columns are modeled as cantilever elements with non-linear behavior. Finally, in addition to the previous considerations, it should be highlighted that the choice of using a simplified structural model derives from the need to have a limited number of representative parameters, that could be more suited for an expeditious probabilistic estimation of structural-vulnerability-induced economic losses.

The Equations of Motions (EoMs) of the system are

$$M\ddot{x}_v(t) + C_v \dot{x}_v(t) + K_v x_v(t) = -Ma_{\lambda,v}(T_R, t) \quad (6a)$$

$$M\ddot{x}_h(t) + C_h \dot{x}_h(t) + K_h x_h(t) = -Ma_{\lambda,h}(T_R, t) + F_f \quad (6b)$$

The EoMs describe the behavior of the system in the vertical and horizontal directions, respectively.  $M$  is the mass of the beam and of the roof system,  $C$  is the damping coefficient,  $K$  is the stiffness,  $a_{\lambda}(T_R, t)$  is the ground-motion time history (Section 2.1) and  $F_f$  is the friction force. The subscripts v and h indicate that the variable is related to the vertical and horizontal direction, respectively.

Eq. (6a) is a second-order linear differential equation and is uncoupled with Eq. (6b). The vertical stiffness is that of a simply supported beam

$$K_v = K_{v,l} + K_{v,r} = \frac{48EI_b}{L^3} \quad (7)$$

where  $E$  is the Young's modulus of the material,  $I_b$  and  $L$  are the area moment of inertia and the length of the beam, respectively. The subscripts  $l$  and  $r$  indicate that the variable is related to the left and right side, respectively.

The vertical support reactions of the beam are

$$R_{v,l}(t) = R_{v,r}(t) = \frac{Mg}{2} + \frac{24EI_b}{L^3} x_v(t) \quad (8)$$

where  $R_{v,l}(t)$  is the vertical support reaction,  $g$  is the gravity acceleration and  $x_v(t)$  is the displacement of the middle of the beam. The first term of Eq. (8) is the static part of the vertical supports reaction while the second term is the dynamic part.

Eq. (6b) is a second-order nonlinear differential equation. Eq. (6b) can be solved after the solution of Eq. (6a) because  $F_f$  is expressed as a function of vertical support reactions of the beam (i.e., Eq. (8)). The nonlinearity is due to the friction and to the nonlinear horizontal stiffness. The stiffness,  $K_h$ , is generated by the parallel connection of the support system of the left and the right side. Each support system consists of the series connection of three sub-elements that represent the mechanical behavior of the foundation, of the column and of the column-to-beam connection system. The horizontal stiffness is

$$K_h = K_l + K_r = \left( \frac{1}{K_{f,r}} + \frac{1}{K_{p,r}} + \frac{1}{K_{c,r}} \right)^{-1} + \left( \frac{1}{K_{f,l}} + \frac{1}{K_{p,l}} + \frac{1}{K_{c,l}} \right)^{-1} \quad (9)$$

where  $K_l$  is the stiffness of the left side support system,  $K_r$  is the stiffness of the right side support system,  $K_f$  is the stiffness of the foundation,  $K_p$  is the stiffness of the column and  $K_c$  is the stiffness of the beam-to-column connection.

After the solution of Eq. (6b), the displacement of each element is evaluated using the partition formula

$$x_{i,j}(t) = x_h(t) \left[ \frac{K_{i,j}^{-1}}{\sum_i K_{i,j}^{-1}} \right] \text{ with } i \in \{f, p, c\}, j \in \{l, r\} \quad (10)$$

where  $x_{i,j}(t)$  is the displacement of the element  $i$  of the portal on its  $j$  (left or right) side.

The force of the foundation and column elements can be evaluated as

$$F_{i,j}(t) = F_j(t) = F(t) \frac{K_j}{K_h} \text{ with } i \in \{f, p\}, j \in \{l, r\} \quad (11)$$

In Eq. (11) the force is divided between the two sides (connected in parallel) and assumes the same values on each element of one side (connected in series).

The foundation is described by a rocking model in which the lateral stiffness at the top of the column is

$$K_{f,j}(t) = \frac{K_{f,r,j}}{H^2} \text{ with } j \in \{l, r\} \quad (12)$$

where  $H$  is the height of the column and  $K_{f,r}$  is the rotational stiffness of the rocking spring located at the base of the foundation.

The foundations and the columns can be described using two types of material models: elasto-plastic or rigid-plastic. Both constitutive laws are described by bilinear function (Fig. 3(a) and 3(b)). In this way, many aspects of the complex behavior of a reinforced concrete element are neglected because such refined modeling does not fall within the scope of this study. The stiffness of each element is evaluated as

$$K_{i,j} = \begin{cases} K_{el,i,j} & \text{if } \{|F_{i,j}| < F_{y,i,j}\} \text{ or } \{|F_{i,j}| \geq F_{y,i,j} \text{ and } \text{sign}(F_{i,j})\dot{x}_{i,j} < 0\} \\ K_{pl,i,j} & \text{if } \{|F_{i,j}| \geq F_{y,i,j} \text{ and } \text{sign}(F_{i,j})\dot{x}_{i,j} \geq 0\} \end{cases} \quad (13)$$

where  $K_{i,j}$  is the tangent stiffness,  $K_{el,i,j}$  is the elastic stiffness,  $K_{pl,i,j}$  is the plastic stiffness and  $F_{y,i,j}$  is the yield force. In Eq. (13), the stiffness of each element is a function of force, of displacement and of velocity. The plastic contribution of the foundations is due to non-reversible deformation of the ground while that of the columns is due to the formation of plastic hinges at the base. These mechanisms correspond with those referred in ReLUIS *et al.* (2012).

The forces acting on the two elements of the connection (connected in parallel) are

$$F_{c,j}(t) = F_j(t) - F_{f,j}(t) \text{ with } j \in \{l, r\} \quad (14)$$

where  $F_c(t)$  is the force on the elasto-plastic part of the connection representing the dowel action in the connection and its stiffness is defined according to Eq. (13). The friction in the connection is based on a mechanism of shear transfer across discontinuities characterized by large variability of the parameters describing the response. In precast structures, friction as a load transfer mechanism was demonstrated experimentally by performing a series of tests on the effectiveness of pure friction as a load path (Foerster *et al.* 1989, Magliulo *et al.* 2011, Zoubek *et al.* 2013). Foerster *et al.* (1989) found that the friction is characterized by an initial slip or static friction load directly proportional to the axial force and by a sliding resistance that is lower. They also investigated the effect of pre-cracking on the friction load path. The pre-cracked interface does not experience the difference between the static friction load and sliding resistance, which are the same. The most common model employed is the Coulomb friction model (Fig 3(c)), which can be formulated as

$$K_{f,j} = \begin{cases} \infty & \text{if } \{|F_{f,j}| < \mu_j R_{v,j}\} \text{ or } \{|F_{f,j}| \geq \mu_j R_{v,j} \text{ and } \text{sign}(F_{f,j})\dot{x}_{f,j} < 0\} \\ K_{c,j} & \text{if } \{|F_{f,j}| \geq \mu_j R_{v,j} \text{ and } \text{sign}(F_{f,j})\dot{x}_{f,j} \geq 0\} \end{cases} \quad (15)$$

where  $F_{f,j}$  is the friction force,  $\dot{x}_{f,j}$  is the sliding velocity and  $\mu$  is the friction coefficient. Eq. (15) defines two distinct behaviors of the connection depending on the excitation level: *non-slip mode* and *slip mode*. In this model, the interface is considered as cracked (Foerster *et al.* 1989) hence it is assumed that the static and dynamic friction coefficients are the same. Moreover, it is assumed that the displacement of the spring ( $K_{c,j}$ ) and the sliding of the friction surface ( $F_{f,j}$ ) are the same since they are in parallel (see Fig. 2(b)). Indications of the value of the friction coefficient in the beam-to-column connections of Italian

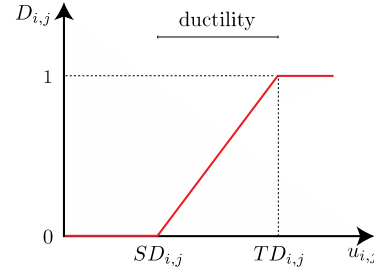


Fig. 4 Example of damage function

precast industrial buildings can be found in Magliulo *et al.* (2011).

The solutions of Eq. (6a) and (6b) are evaluated using the Newmark method (Newmark 1959). The solutions of Eq. (6a) and (6b) are evaluated for each of the 7 ground-motion time histories described in Section 2.1.

### 2.3 Damage and collapse estimation

The economic loss estimation requires the definition of the structural damage as a function of the seismic input, i.e., vulnerability. In this study, the damage is evaluated using the maximum displacement of each element found during the non-linear analyses

$$u_{i,j} = \max_t u_{i,j}(t) \quad (16)$$

The damage is estimated using linear functions (Fig. 4)

$$D_{i,j} = \begin{cases} 0 & \text{if } u_{i,j} \leq SD_{i,j} \\ \frac{u_{i,j} - SD_{i,j}}{TD_{i,j} - SD_{i,j}} & \text{if } SD_{i,j} < u_{i,j} < TD_{i,j} \\ 1 & \text{if } u_{i,j} \geq TD_{i,j} \end{cases} \quad (17)$$

where  $D_{i,j}$  is the damage function that varies between 0 (element completely undamaged) and 1 (element completely damaged, i.e., failure),  $SD_{i,j}$  is the displacement at which the element starts to be damaged, which can be evaluated for both foundations and columns as the yield displacement

$$SD_{i,j} = \frac{F_{y,i,j}}{K_{el,i,j}} \quad (18)$$

and  $TD_{i,j}$  is the displacement at which the element is fully damaged. The damage function of the connection is always described by Eq. (17), but in this case  $SD_{c,j}$  and  $TD_{c,j}$  are described as characteristics of the connection. In particular, the value of  $SD_{c,j}$  is associated with the level of displacement that produces damage of the connection due to the sliding (i.e., need of repair works for the repositioning of the beam on the columns). The complete damage,  $TD_{c,j}$ , occurs when sliding exceeds the limit imposed by the connection and the beam loses its support (i.e., loss of support condition).

As for the damage, the collapse is usually described by collapse fragility curves (Nutti *et al.* 2004, 2009, Jaiswal *et al.* 2011). The definition of collapse in this study is when one structural component is completely damaged, i.e.,  $D_{i,j}=1$ . In the case of statically determined structures, like

precast industrial buildings, this is a reasonable assumption. In fact, failure of one element implies at least a local collapse, possibly leading to a global one. Accordingly, in this study the collapse is described using a collapse function

$$CL = \begin{cases} 0 & \text{if } D_{i,j} < 1 \text{ for all } i \in \{f, p, c\}, j \in \{l, r\} \\ 1 & \text{otherwise} \end{cases} \quad (19)$$

The collapse function assumes the values 0 for non-collapsed structure and 1 for collapsed structure.

#### 2.4 Economic losses estimation

The economic consequences of earthquakes may occur both before and after the seismic event itself (Dowrick 2009). The focus of this study is on those occurring after earthquakes.

Economic losses relative to a single industrial building can be classified into stock and flow losses. Stock refers to a quantity at a single point in time, whereas flow refers to services or outputs of stocks over time (Rose 2004). Following these definitions, property damage represents a decline in stock value while business interruptions losses are a flow measure.

In this study, higher-order losses are neglected as only direct structural-vulnerability-induced economic losses are considered. Moreover, economic losses deriving from subsequent shocks on the same damaged structure are neglected (e.g., Der Kiureghian 2005) and only economic losses for each occurrence are evaluated.

The economic losses are the sum of three contributions

$$TL = RL + SL + FL \quad (20)$$

where  $TL$  are the total losses,  $RL$  are the repair losses,  $SL$  are the stock losses and  $FL$  are the flow losses.

The repair losses are evaluated as

$$RL = \begin{cases} \sum_i \sum_j D_{i,j} RC_{i,j} & \text{if } CL = 0 \\ RTC & \text{if } CL = 1 \end{cases} \quad (21)$$

where  $RC_{i,j}$  is the maximum repair cost of the element and  $RTC$  is the repair total cost representing the building value plus additional costs related to demolition and debris removal in case of collapse. According to Eq. (21), a linear relationship between the damage level and the repair cost is adopted. Repair costs concern the repair and retrofitting costs of the damaged structural elements.

The stock losses are evaluated as

$$SL = \begin{cases} 0 & \text{if } CL = 0 \\ SV & \text{if } CL = 1 \end{cases} \quad (22)$$

where  $SV$  is the stored value representing the value of goods stored inside the building during the seismic event.  $SV$  is strongly variable in time, e.g., in an industrial warehouse building of a shipping company, the value of goods stored varies with daily frequency due to loading and unloading. In this model, it is assumed that damage to the contents will take place only if the collapse occurs (Eq. (22)). Clearly, damage to property contained in the building may also occur for other reasons such as overturning of cabinets and equipment that are typically related to the input seismic

accelerations or the collapse of claddings. These will not be considered in the following because the focus of this study is structural-vulnerability-related economic losses. Other economic losses related to damage or collapse of non-structural elements (e.g., cladding, cabinets, cranes, equipment, etc.), although of remarkable importance, do not fall within the scope of this study because they cannot be easily generalized and, rather, deserve a case-by-case approach considering the specificity of the content.

The flow losses are evaluated as

$$FL = \begin{cases} \sum_i \sum_j NDL \cdot \left[ \max_i \max_j D_{i,j} RT_{i,j} \right] & \text{if } CL = 0 \\ NDL \cdot TRT & \text{if } CL = 1 \end{cases} \quad (23)$$

where  $NDL$  is the net day loss representing the costs per working day due to interruption in terms of loss of earnings and expenses that cannot be canceled during the repair of the structure (e.g., wages),  $RT_{i,j}$  is the maximum repair time of each element expressed in days and  $TRT$  is the total repair time and represents the time of demolition and reconstruction of the building in case of collapse. In this model, it is assumed a linear relation between the level of damage and the repair time. It is also assumed that repair operations on different elements can be carried out simultaneously, implying that the repair time is equal to the maximum time that any element requires to be repaired.

#### 2.5 Monte Carlo simulation and probability of structural-vulnerability-induced economic losses

The procedure followed in the evaluation of the structural-vulnerability-induced economic losses by means of Monte Carlo simulations is as follows (Fig. 1):

- definition of the location of the building;
- generation of 9 groups of 7 sets of ground-motion time histories (using the elastic spectra given in the Italian Building Code (NTC-2008, 2008) for the location of the building), corresponding to  $T_{R,m}=30, 50, 72, 101, 140, 201, 475, 975, 2475$  years;
- generation of  $N$  input values of  $T_R$ , randomly chosen from the probability distribution in Eq. (5) having fixed  $V_R$ ;
- selection of  $N$  sets of ground-motion time histories from the input values of  $T_R$  using Eq. (4) and the 9 groups of 7 sets previously generated;
- generation of  $N$  input parameters (dynamic model, damage model and loss model described in Sections 2.2, 2.3 and 2.4) randomly from defined probability distributions;
- deterministic computations of the maximum dynamic response, damage and of the economic losses using the generated inputs;
- evaluation of the probability of structural-vulnerability-induced economic losses for each occurrence from the outcomes of the deterministic computations.

Following this procedure, the probability of structural-vulnerability-induced economic losses associated with a single event during the time period,  $V_R$ , is computed. This parameter is of primary importance for the definition of the insurance premiums (i.e., the amount of money to be

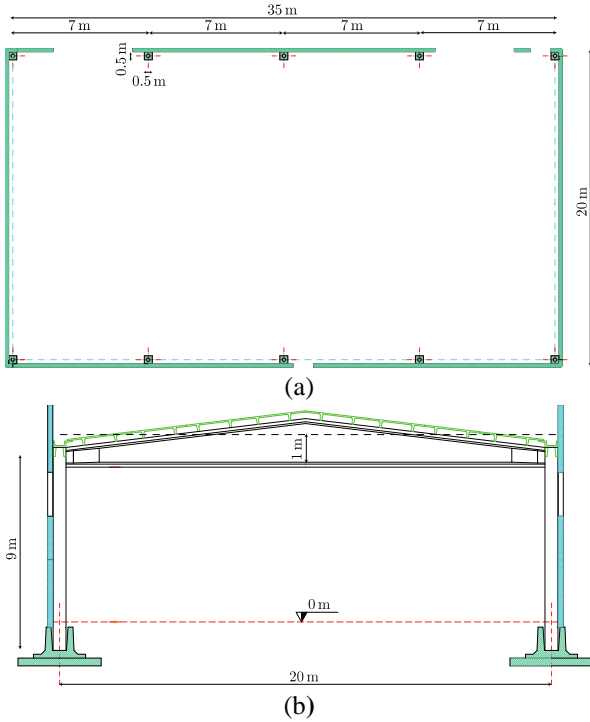


Fig. 5 (a) Plan of the building, (b) Section of the building

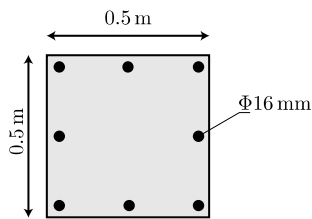


Fig. 6 Cross-section and reinforcement of the columns

charged for a certain amount of insurance coverage) (Grossi 2005).

Insurance companies can define the limit of indemnity and the excess: these are the upper and lower limit of the indemnity, respectively. The limit of indemnity is the maximum amount an insurer will pay in respect of any one claim first made against the insured and notified to the insurer during the policy period. The excess (or deductible) is that part of a claim that remains uninsured and is achieved by a policy condition requiring the insured to pay the first portion of a loss in respect of any one claim, with the insurer settling the balance above the excess up to the limit of indemnity. The variation of these two limits in the insurance policy terms, on one hand can vary the premium and on the other hand can modify the risk of loss for the insured. Using the probability of economic losses associated with a single event, owners can evaluate the risk associated with a single event given the insurance policy terms. Moreover, insurance companies can use the outcomes of this framework in the preliminary definitions of policy terms.

### 3. Numerical example of economic loss estimation

To illustrate the economic loss estimation procedure, a prototype single-story single-bay industrial building located

in Mirandola, Italy, was designed and analyzed. The prototype building represents a precast industrial building located in the Emilia-Romagna area hit by the earthquake of 2012. The parameters adopted in this example are qualitative values and representative of this typology of buildings, mainly chosen using reasonable engineering judgment criteria. The economic parameters are estimated using reference values that are reasonable for the Italian territory at the time when this paper was written. In the following, all the parameters and their probability distributions are presented.

Parameter	Mean value	Probability distribution
$M$	52000 kg	$\mathcal{N}(\mu, \sigma^2)$
$\xi_h$	2%	$\mathcal{N}(\mu, \sigma^2)$
$\xi_v$	2%	$\mathcal{N}(\mu, \sigma^2)$
$K_v$	6260 kN/m	$\mathcal{N}(\mu, \sigma^2)$

The prototype building is single-story and single-bay with 5 precast concrete frames. The plan of the shed is shown in Fig. 5(a) and the vertical section in Fig. 5(b). The building is rectangular and measures 20×35 m in plan and has a height of approximately 9 m. The building area is 700 m<sup>2</sup>.

9 groups of 7 horizontal and vertical ground-motion time histories were generated using SIMQKE for  $T_{R,m}=30, 50, 72, 101, 140, 201, 475, 975, 2475$  years, using as input elastic response spectra for Mirandola given in the Italian Building Code (NTC-2008, 2008) for soil type C that is a typical soil class of the Emilia Romagna area (e.g., Vanzi *et al.* 2015) and topographic class T1.

$N=10^4$  inputs values of  $T_R$  were generated using randomly the exponential probability distribution in Eq. (5) with  $V_R=50$  years. Using the 9 groups previously generated,  $N=10^4$  groups (Section 3.1) of time histories were selected from the inputs values of  $T_R$  using Eq. (4).

The parameters and the probability distribution adopted in the Monte Carlo analysis are reported in Tables from 1, to 5. In the following, these are presented and discussed. The mass,  $M$ , is the sum of the beam and of the roof system masses. It was evaluated considering the specific weight of the beam equal to 2500 kg/m<sup>3</sup> (reinforced concrete density) and the weight per unit area the roof system equal to 200 kg/m<sup>2</sup>. Viscous damping equal to  $\zeta=2\%$  was assumed both in vertical and horizontal directions (Pant *et al.* 2013).

The vertical stiffness was estimated according to Eq. (7)

$$K_v = K_{v,l} + K_{v,r} = \frac{48EI_b}{L^3} = 6260 \frac{kN}{m} \quad (24)$$

where  $E=2.5 \times 10^{10}$  N/m<sup>2</sup> is the elastic modulus of the concrete,  $I_b=4.17 \times 10^{-2}$  m<sup>4</sup> is the moment of inertia of the beam evaluated considering the section constant with dimension equal to the average dimension 0.5×1 m and  $L=20$  m is the length of the beam. The mass, damping ratios and vertical stiffness were modelled using Normal probability distributions,  $\mathcal{N}(\mu, \sigma^2)$ . The input parameters

Table 2 Mechanical parameters of the support system in horizontal direction

	Left		Right		Probability distribution
	Parameter	Mean value	Parameter	Mean value	
Foundation	$K_{el,f,l}$	658 kN/m	$K_{el,f,r}$	658 kN/m	$\mathcal{N}(\mu, \sigma^2), \rho(l, r) = 0$
	$K_{pl,f,l}$	/	$K_{pl,f,r}$	/	$\mathcal{N}(\mu, \sigma^2), \rho(l, r) = 0$
	$F_{y,f,l}$	$\infty$	$F_{y,f,r}$	$\infty$	$\mathcal{N}(\mu, \sigma^2), \rho(l, r) = 0$
Column	$K_{el,p,l}$	138 kN/m	$K_{el,p,r}$	138 kN/m	$\mathcal{N}(\mu, \sigma^2), \rho(l, r) = 0$
	$K_{pl,p,l}$	62.5 kN/m	$K_{pl,p,r}$	62.5 kN/m	$\mathcal{N}(\mu, \sigma^2), \rho(l, r) = 0$
	$F_{y,p,l}$	18 kN	$F_{y,p,r}$	18 kN	$\mathcal{N}(\mu, \sigma^2), \rho(l, r) = 0$
Connection	$K_{el,c,l}$	5 kN/m	$K_{el,c,r}$	5 kN/m	$\mathcal{N}(\mu, \sigma^2), \rho(l, r) = 0$
	$K_{pl,c,l}$	/	$K_{pl,c,r}$	/	$\mathcal{N}(\mu, \sigma^2), \rho(l, r) = 0$
	$F_{y,c,l}$	/	$F_{y,c,r}$	/	$\mathcal{N}(\mu, \sigma^2), \rho(l, r) = 0$
	$\mu_l$	0.2	$\mu_r$	0.2	$\mathcal{N}(\mu, \sigma^2), \rho(l, r) = 0$

Table 3 Damage parameters

	Left		Right		Probability distribution
	Parameter	Mean value	Parameter	Mean value	
Foundation	$SD_{f,l}$	/	$SD_{f,r}$	/	/
	$TD_{f,l}$	/	$TD_{f,r}$	/	/
Column	$SD_{p,l}$	0.13 m	$SD_{p,r}$	0.13 m	/
	$TD_{p,l}$	0.22 m	$TD_{p,r}$	0.22 m	$\mathcal{N}(\mu, \sigma^2), \rho(l, r) = 0$
Connection	$SD_{c,l}$	0.1 m	$SD_{c,r}$	0.1 m	$\mathcal{N}(\mu, \sigma^2), \rho(l, r) = 0$
	$TD_{c,l}$	0.2 m	$TD_{c,r}$	0.2 m	$\mathcal{N}(\mu, \sigma^2), \rho(l, r) = 0$

Table 4 Economic loss parameters (Data are referred to a single span of the structure)

	Left		Right		Probability distribution
	Parameter	Mean value	Parameter	Mean value	
Foundation	$RC_{f,l}$	12,000 €	$RC_{f,r}$	12,000 €	$\mathcal{N}(\mu, \sigma^2), \rho(l, r) = 1$
	$RT_{f,l}$	60 days	$RT_{f,r}$	60 days	$\mathcal{N}(\mu, \sigma^2), \rho(l, r) = 1$
Column	$RC_{p,l}$	8,000 €	$RC_{p,r}$	8,000 €	$\mathcal{N}(\mu, \sigma^2), \rho(l, r) = 1$
	$RT_{p,l}$	40 days	$RT_{p,r}$	40 days	$\mathcal{N}(\mu, \sigma^2), \rho(l, r) = 1$
Connection	$RC_{c,l}$	4,000 €	$RC_{c,r}$	4,000 €	$\mathcal{N}(\mu, \sigma^2), \rho(l, r) = 1$
	$RT_{c,l}$	20 days	$RT_{c,r}$	20 days	$\mathcal{N}(\mu, \sigma^2), \rho(l, r) = 1$

were the mean,  $\mu$ , equal to the mean values, and the variance,  $\sigma^2$ , evaluated using a coefficient of variation,  $c_v = \sigma/\mu$ , equal to 5% for the mass, 20% for the damping and 10% for the stiffness. The lowering of the coefficient of variation is estimated according to the uncertainties associated with the variable.

The elastic stiffness of the foundation was evaluated considering the foundation as rigid on an elastic soil described by the modulus of sub-grade reaction,  $k_s$ . The stiffness of the foundations is

$$K_{el,f,l} = K_{el,f,r} = \frac{k_s \cdot I_{f,j}}{H^2} = 658 \frac{kN}{m} \quad (25)$$

where  $k_s = 4 \times 10^4 \text{ kN/m}^3$  is the modulus of sub-grade reaction for clayey medium dense sand (Bowles 1988) and  $I_{f,j} = 1.33$

$\text{m}^4$  is the moment of inertia of the base foundation that is  $2 \times 2 \text{ m}$ .

The columns behavior was evaluated considering the reinforcement bars described by a bilinear stress–strain relationship both in tension and compression and the concrete behavior described by the parabolic-rectangular stress block. The yielding stress of the steel is 430 MPa and the concrete strength is 40 MPa. The columns have a cross-section of  $0.5 \times 0.5 \text{ m}$ ; the reinforcement is given in Fig. 6. The stiffness was estimated accounting for an axial load on the columns equal to half of the mass neglecting the dynamic part of the vertical load.

The friction coefficient (neoprene-to-concrete) was set equal to 0.2 (Magliulo *et al.* 2011). The dowel was modeled as an elastic element with stiffness equal to 5 kN/m.

All the mechanical parameters were modeled using Normal probability distributions,  $\mathcal{N}(\mu, \sigma^2)$ . The input parameters were the mean equal to the mean values and the variance evaluated using a coefficient of variation,  $c_v = \sigma/\mu$ , equal to 10% and only for the friction coefficient of 20%. It must be mentioned that no correlation was given between the variables of the left and right side,  $\rho(l, r) = 0$ , assuming that the elements of the two sides may have different mechanical characteristics in the random sampling of the Monte Carlo analysis.

The displacement at which the column starts to be damaged and at which the column is completely damaged were evaluated performing a pushover analysis of the column using a model with distributed plasticity and displacement-based formulation. These were found to be equal to 0.13 m and 0.22 m, respectively. These values correspond to the first yielding of the material and to the ultimate condition of the cross-section, respectively.

The displacement at which the connection starts to be damaged was evaluated equal to 0.1 m, and the displacement at which the connection is completely damaged was estimated 0.2 m. In particular, the first value is considered as the minimum displacement requiring repair works for the repositioning of the beam on the column, while the second was assumed considering a support length equal to half of the column cross-section, i.e., 0.25 m, and a minimum required support length of 0.05 m. It should be highlighted that in general, the support length can be much lower than half column cross-section leading to a lower capacity of the beam-to-column connection.

For the foundations, these quantities are not defined because the plastic behavior is not considered consequently ignoring damage phenomena. All the damage parameters were modeled using Normal probability distributions,  $\mathcal{N}(\mu, \sigma^2)$ . The input parameters were the mean equal to the mean values and the variance evaluated using a coefficient of variation equal to 10%. No correlation was assumed between the variables of the left and right sides.  $SD_{p,j}$  is considered as a deterministic parameter expressed in terms of the random mechanical parameters as reported in Eq. (18). Accordingly, in Table 3,  $SD_{p,j}$  has no probability distribution.

The maximum repair cost of the foundation was estimated in 12,000 €, of the column in 8,000 € and of the connection in 4,000 €. The repair cost of the foundation is given even though it is not accounted for damage (Table 3).

Table 5 Economic loss parameters of the entire building (Data are referred to the entire structure)

Parameter	Mean value	Probability distribution
RTC	340,000 €	$\mathcal{N}(\mu, \sigma^2)$
TRT	180 days	$\mathcal{N}(\mu, \sigma^2)$
NDL	1,000 €/day	$\mathcal{N}(\mu, \sigma^2)$
SV	350.000 €	$\mathcal{U}(a, b)$

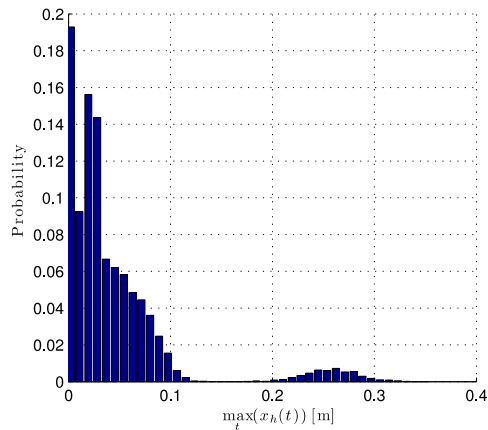


Fig. 7 Probability distribution of the estimated maximum horizontal beam displacement

The lowering of the cost is estimated according to the complexity of the repair work. It must be highlighted that costs are related to a single element, therefore they are multiplied times 5 (the number of element for side, Fig. 5(a), in order to obtain the total loss of the building. The sum of maximum repair costs of all the elements is 240,000 €; this value is lower than the repair total cost, RTC, as it represents the limiting case of repair cost of the entire structure and not account for the reconstruction of the same.

The maximum repair time of the foundation is estimated in 60 days, of the column in 40 days and of the connection in 20 days. Even in this case, the lowering of the repair time is estimated according to the complexity of the repair work. The repair total cost is estimated considering a price per square meter of 400 €/m<sup>2</sup> and the cost of demolition equal to 60,000 €. The net day loss is set equal to 1,000 €/day and it was assessed using a reasonable value for a business carried out in a building of this size. The total repair time was estimated to be half year. The stored value was estimated at 500 €/m<sup>2</sup>. Complete correlation was assumed between the variables of the left and right side to the probability distributions of Table 4, i.e.,  $\rho(l,r)=1$ .

The coefficients RTC and NDL (Table 5) were modeled using Normal probability distributions,  $\mathcal{N}(\mu, \sigma^2)$  with a coefficient of variation equal to 30%. The large values of the coefficients of variation are associated with a strong uncertainty in the evaluation of these parameters, especially considering the post-earthquake scenario. Differently, SV was modeled using a uniform distribution,  $\mathcal{U}(a, b)$ . The input parameters were the minimum, a, and maximum, b, values that were assumed as 0 € and twice the mean values, 700,000 €. This strong variability in the stored value

parameter is adopted to model scenarios characterized by different amounts of goods stored inside the building (e.g., a warehouse wherein the amount of contained goods frequently varies for load and unload of goods) and by modification of the internal use (and related content) of the industrial building during the exposure period.

### 3.1 Monte Carlo simulation results

Using the parameters and the probability distributions reported above, a Monte Carlo simulation was performed using the procedure reported in Section 2.5. The results of the Monte Carlo analyses are shown in Figs. 7 and 8 in terms of probability distributions of the maximum horizontal displacement of the beam and of estimated earthquake structural-vulnerability-induced economic losses for each occurrence (i.e., seismic event), respectively.

Fig. 7 shows the probability distribution of the estimated maximum horizontal beam displacement,  $x_h$  (Fig. 2(b)). The distribution obtained is bimodal appearing two distinct peaks; this typically represents the outcomes of two processes with different probability distributions combined in one set of data. The two modes of the probability distribution are unequal and the major mode represents the elastic response of the structure, while the minor mode represents the inelastic response. This was verified by evaluating the two probability distributions in the case of activation of the nonlinear mechanisms (activation of the plastic hinges in the columns and/or activation of the slip mode in the connection). When the nonlinear behavior of the structure is activated, a drop corresponding to an increase of the displacement response as compared with the same structure during the linear behavior is observed; this is due to the stiffness reduction. Moreover, it was observed that the majority of the beam displacement during the nonlinear response depends on the connection for the friction mechanism although this result strongly depends on the coefficient of friction adopted. Accordingly, the major mode is characterized by seismic events of low intensity and high frequency of occurrence that produce forces of low intensity unable to activate nonlinear mechanisms. The two modes are separated by a gap. The gap is approximately located at  $\max x_h(t)=0.15$  m. After the gap, the minor mode is characterized by seismic events of high intensity and low frequency of occurrence that produce forces of large intensity able to activate nonlinear mechanisms. The peak of the minor mode is approximately at  $\max x_h(t)=0.27$  m. For some combinations of parameters, the Monte Carlo analysis predicts maximum horizontal displacements up to 1 m although the showed range of the axis  $\max x_h(t)$  in Fig. 7 is [0,0.4]. As a matter of fact, values of displacement over 0.3 m are characterized by a really low probability of occurrence, as visible in Fig. 7.

Fig. 8(a) shows the probability distribution, the Cumulative Distribution Function (CDF) and the Complementary CDF of the estimated earthquake economic losses for each occurrence (i.e., seismic event) expressed in millions of Euros within the time period  $V_R=50$  “years”. Also in this case, the obtained probability distribution is bimodal. The two modes are not comparable in terms of probability of occurrence. The major mode represents the

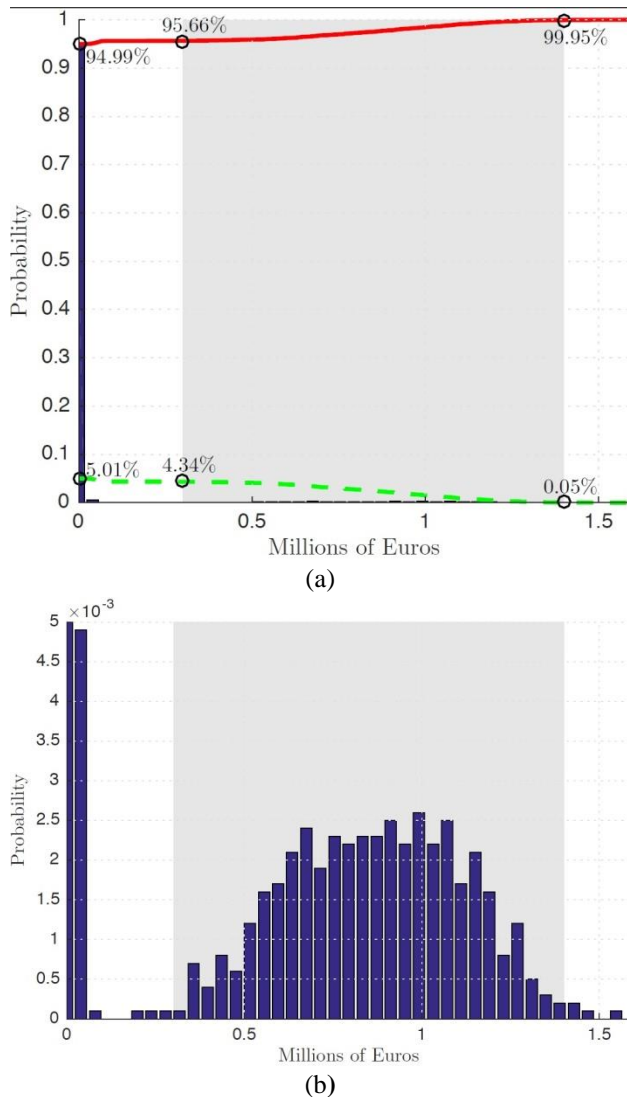


Fig. 8 Probability distribution, CDF (red line) and Complementary CDF (dashed green line) of the estimated earthquake economic losses for each occurrence in € within the time period  $V_R=50$  years (a) and detail of the probability distribution reported in 8(a). Grey-hatched area indicates the assumed range of indemnity of an insurance policy: the limit of indemnity and the excess are 1.4 and 0.3 millions of Euros, respectively.

condition of no occurrence of earthquake economic losses, i.e., zero economic losses. The cumulative probability (i.e., the area under the probability distribution in the range around zero economic losses) is approximately 95% (see red line in Fig. 8(a)). The complementary probability is 5% and gives the cumulative probability of occurring of earthquake economic loss (see green line in Fig. 8(a)). The CDF and the Complementary CDF (Fig. 8(a)) reaches the cumulative probability equal to 1 or 0, respectively, for an economic loss of 1.6 millions of Euros. The two modes are separated by a gap. The gap is approximately located at 0.2 millions of Euros. The minor mode represents the condition of economic-losses occurrence.

In order to better appreciate the values of the probability of the minor mode, in Fig. 8(b) the probability distribution

reported in Fig. 8(a) is plotted in the range of probability  $[0.5 \times 10^{-3}]$ . The earthquake economic losses associated with larger probability of occurrence are in the range of 0.6 and 1.2 millions of Euros and are roughly characterized by a constant probability of approximately  $2 \times 10^{-3}$  (Fig. 8(b)). This mode is the combination of the scenarios of local repair and total reconstruction of the building; this is due to the selected parameters producing two overlapped probability distribution represented by a single mode. In low earthquake shaking intensities, earthquake economic losses are related to the repair time and cost of the damage on each element. At higher shaking intensities, the first structural component failure causes collapse that generates high economic losses deriving from the value of the building plus additional costs related to demolition and debris removal and the destruction of the stored goods.

The complementary CDF reported in Fig. 8(a) (green line) shows the probability of exceeding given an earthquake economic loss value; it should be highlighted that the area underneath the complementary CDF is the average loss and can be used as a scalar measure to compare different designs and has relevance to the premium one would be willing to pay to insure the building against the direct earthquakes economic losses (Yang *et al.* 2009). In this case, the area underneath the complementary CDF is equal to 39,024 €. Moreover, the Probable Maximum Loss (PML) is another important indicator adopted in insurance practice to define losses under a significant seismic event with a certain probability of exceedance for a portfolio of structures in a given time period (Grossi 2005). PML can be evaluated with the Complementary CDF of the estimated earthquake economic losses for each occurrence in € within the time period  $V_R=50$  years reported in Fig. 8(a). The insurer can use the Complementary CDF curve to determine how large a loss will occur fixed a probability level. For example, suppose that an insurer specifies its acceptable risk level as the 1% probability of exceedance. From Fig. 8(a), it can be seen that the 1%-PML is approximately 1.1 millions of Euros.

### 3.2 Example of an insurance policy

Finally, in order to understand the use of probability distribution of the estimated earthquake economic losses for each occurrence in order to define the financial risk for the insurer and the owner (i.e., insured), a hypothetical insurance policy is analyzed: it will be supposed to have an insurance policy with the limit of indemnity and the excess equal to 1.4 and 0.3 millions of Euros, respectively (grey-hatched area in Fig. 8).

The risk for the owner is referred to three scenarios: (1) no losses, (2) losses related to the excess and (3) losses related to the limit of indemnity. In particular, (1) the owner will not pay for earthquake economic losses for each occurrence in the 94.99% of the cases, i.e., when no losses occur. Differently, (2) the owner will pay at most 0.3 millions of Euros (i.e., related to the excess) in the 4.96% of the cases, i.e., cumulated probability in the range of losses (0 €,  $1.4 \times 10^6$  €). Finally, (3) the owner will pay at most 0.5 millions of Euros (i.e., 0.3 millions of Euros added to 0.2

millions of Euros related to the excess and to the limit of indemnity, respectively) in the 5.01% of the cases, i.e., cumulated probability in the range of losses (0 €,  $1.6 \times 10^6$  €). However, only in the 0.05% of the cases, the owner will pay for losses exceeding the limit of indemnity.

The risk for the insurer is referred to two scenarios: (1) losses lower than the excess and (2) losses between the excess and the limit of indemnity. In particular, (1) the insurer will not pay for earthquake economic losses for each occurrence in the 95.66% of the cases, i.e., when losses lower than the excess occur. Differently, (2) the insurer will pay at most 1.1 millions of Euros (i.e., differences between the limit of indemnity and the excess) in the 4.34% of the cases, i.e., cumulated probability in the range of losses ( $3 \times 10^5$  €,  $1.6 \times 10^6$  €). Finally, the insurer will not pay for earthquake economic losses larger than the 1.4 millions of Euros, i.e., the limit of indemnity, covering only 1.1 millions of Euros, differences between the limit of indemnity and the excess.

Finally, it should be highlighted that increasing the difference between the limit of indemnity and the excess, the risk for the owner is reduced while that one for the insurer is increased although this corresponds to an increase of the premium for the owner. A correct strategy of risk management should balance the limit of indemnity and the excess between costs and risks (e.g., Grossi 2005, Paudel *et al.* 2015). Moreover, these results can be used for risk allocation optimization in a public-private partnership for providing insurance coverage for earthquakes available at an affordable price (Paudel *et al.* 2015).

#### 4. Conclusions

A simplified framework for the probabilistic estimation of economic losses induced by the structural vulnerability in single-story and single-bay precast industrial buildings is presented. The economic losses are evaluated considering seismic hazard, structural response, damage resulting from the structural vulnerability and only structural-vulnerability-induced economic losses, i.e., structural repair or reconstruction costs (stock and flow costs) and content losses induced by structural collapse. The uncertainties associated with each of these parts is accounted for via Monte Carlo simulations.

A prototype one-story single-bay concrete precast industrial building located in Mirandola, Italy, is used as an example to illustrate the economic loss estimation outcomes. The structural and economic parameters adopted are representative of this typology of buildings in Italy. The results show that the probability distribution of the maximum displacement of the beam has a bimodal distribution (elastic and inelastic response) and that the probability distribution of earthquake economic losses for each occurrence (i.e., seismic event) has a bimodal distribution (no earthquake economic losses and earthquake economic losses of repair and reconstruction).

The insurance policy terms (the limit of indemnity and the excess) are discussed in terms of effects on the risks and costs for the owner and for the insurer. In particular, it is

shown that increasing the difference between the limit of indemnity and the excess (i.e., the range of indemnity of an insurance policy), the risk for the owner is reduced while that one for the insurer increases, although this corresponds to an increase of the premium for the owner.

The application of this framework requires the characterization of a large number of parameters defining the mechanical and economical property of the structure. Real-world applications would also require an accurate estimation of the statistical properties of the parameters involved in the model for this structural typology using readily available data of structural geometrical characteristics (e.g., from rapid exterior survey and/or existing structural drawings). In addition, important applications of the framework are its extension to assessments of earthquake loss estimation at the regional scale and the economic evaluation and the developing of procedures for the optimization of the structural retrofit considering both mechanical and economical results. Further work, currently in progress, is required to investigate these aspects.

#### Acknowledgments

ReLUIS 2014–2018 project, research line 2.1, is acknowledged for the financial support given to the present research.

#### References

- Anagnos, T. and Kiremidjian, A.S. (1988), “A review of earthquake occurrence models for seismic hazard analysis”, *Probabilist. Eng. Mech.*, **3**(1), 3-11.
- Aon Benfield (2013), Annual Global Climate and Catastrophe Report: 2012.
- Asprone, D., De Risi, R. and Manfredi, G. (2016), “Defining structural robustness under seismic and simultaneous actions: an application to precast RC buildings”, *Bull. Earthq. Eng.*, **14**(2), 485-499.
- ATC-58 (2012), *Development of Next-Generation Performance-Based Seismic Design Procedures for New and Existing Buildings*, Applied Technology Council 58.
- Babič, A. and Dolšek, M. (2016), “Seismic fragility functions of industrial precast building classes”, *Eng. Struct.*, **118**, 357-370.
- Bonfanti, C., Carabellese, A. and Toniolo, G. (2008), *Strutture Prefabbricate: Catalogo Delle Tipologie Esistenti*, Milano ASSOBETON.
- Bournas, D.A., Negro, P. and Taucer, F.F. (2014), “Performance of industrial buildings during the Emilia earthquakes in Northern Italy and recommendations for their strengthening”, *Bull. Earthq. Eng.*, **12**(5), 2383-2404.
- Bowles, J.E. (1988), *Foundation Analysis and Design*, McGraw-Hill Book Company Limited, England.
- Braga, F., Gigliotti, R., Monti, G., Morelli, F., Nuti, C., Salvatore, W. and Vanzi, I. (2014), “Speedup of post earthquake community recovery: the case of precast industrial buildings after the Emilia 2012 earthquake”, *Bull. Earthq. Eng.*, **12**(5), 2405-2418.
- Casotto, C., Silva, V., Crowley, H., Nascimbene, R. and Pinho, R. (2015), “Seismic fragility of Italian RC precast industrial structures”, *Eng. Struct.*, **94**, 122-136.
- Colapietro, D., Netti, A., Fiore, A., Fatiguso, F. and Marano, G.C.

- (2014), "On the definition of seismic recovery interventions in R.C. buildings by non-linear static and incremental dynamic analyses", *Int. J. Mech.*, **8**(1), 216-222.
- Cornell, C.A. (1968), "Engineering seismic risk analysis", *Bull. Seismo. Soc. Am.*, **58**(5), 1583-1606.
- Dassori, E. and Assobeton (2001), *La Prefabbricazione in Calcestruzzo: Guida All'utilizzo Nella Progettazione*, Milano ASSOBETON.
- Demartino, C., Monti, G. and Vanzi, I. (2017a), "Seismic loss-of-support conditions of frictional beam-to-column connections", *Struct. Eng. Mech.*, **61**(4), 527-538.
- Demartino, C., Vanzi, I., Monti, G. and Sulpizio, C. (2017b), "Precast industrial buildings in Southern Europe: loss of support at frictional beam-to-column connections under seismic actions", *Bull. Earthq. Eng.*, 1-36.
- Der Kiureghian, A. (2005), "Non-ergodicity and PEER's framework formula", *Earthq. Eng. Struct. Dyn.*, **34**(13), 1643-1652.
- Dowrick, D.J. (2009), *Earthquake Resistant Design and Risk Reduction*, John Wiley & Sons.
- Ercolino, M., Magliulo, G. and Manfredi, G. (2016), "Failure of a precast RC building due to Emilia-Romagna earthquakes", *Eng. Struct.*, **118**, 262-273.
- Foerster, H.R., Rizkalla, S.H. and Heuvel, J.S. (1989), "Behavior and design of shear connections for loadbearing wall panels", *PCI J.*, **34**(1), 102-119.
- Grossi, P. (2005), *Catastrophe Modeling: A New Approach to Managing Risk*, Vol. 25, Springer Science & Business Media.
- Jaiswal, K., Wald, D. and D'Ayala, D. (2011), "Developing empirical collapse fragility functions for global building types", *Earthq. Spec.*, **27**(3), 775-795.
- Jalayer, F. (2003), "Direct probabilistic seismic analysis: implementing non-linear dynamic assessments", Ph.D. Thesis, Stanford University.
- Liberatore, L., Sorrentino, L., Liberatore, D. and Decanini, L.D. (2013), "Failure of industrial structures induced by the Emilia (Italy) 2012 earthquakes", *Eng. Failure Anal.*, **34**, 629-647.
- Magliulo, G., Fabbrocino, G. and Manfredi, G. (2008), "Seismic assessment of existing precast industrial buildings using static and dynamic nonlinear analyses", *Eng. Struct.*, **30**(9), 2580-2588.
- Magliulo, G., Capozzi, V., Fabbrocino, G. and Manfredi, G. (2011), "Neoprene-concrete friction relationships for seismic assessment of existing precast buildings", *Eng. Struct.*, **33**(2), 532-538.
- Magliulo, G., Ercolino, M., Petrone, C., Coppola, O. and Manfredi, G. (2014), "The Emilia earthquake: seismic performance of precast reinforced concrete buildings", *Earthq. Spec.*, **30**(2), 891-912.
- Marzo, A., Marghella, G. and Indirli, M. (2012), "The Emilia-Romagna earthquake: damages to precast/prestressed reinforced concrete factories", *Ingegneria Sismica*, **2**, 132-147.
- Miranda, E. and Aslani, H. (2003), *Building-Specific Loss Estimation Methodology*, Report PEER, 3, 2003.
- Newmark, N.M. (1959), "A method of computation for structural dynamics", *Proc. ASCE*, **85**.
- Nuti, C., Santini, S. and Vanzi, I. (2004), "Damage, vulnerability and retrofitting strategies for the Molise hospital system following the 2002 Molise, Italy, earthquake", *Earthq. Spec.*, **20** (SPEC. 1), S285-S299.
- Nuti, C., Rasulo, A. and Vanzi, I. (2009), "Seismic assessment of utility systems: Application to water, electric power and transportation networks safety, reliability and risk analysis: Theory, methods and applications", *Proceedings of the Joint ESREL and SRA-Europe Conference*, 3, 2519-2529.
- NTC-2008 (2008), Ministerial Decree: "NTC 2008 - Norme tecniche per le costruzioni".
- Pant, D.R., Wijeyewickrema, A.C. and ElGawady, M.A. (2013), "Appropriate viscous damping for nonlinear time-history analysis of base-isolated reinforced concrete buildings", *Earthq. Eng. Struct. Dyn.*, **42**(15), 2321-2339.
- Parisi, F., De Luca, F., Petruzzelli, F., De Risi, R., Chioccarelli, E. and Iervolino, I. (2012), "Field inspection after the May 20th and 29th 2012 Emilia-Romagna earthquakes", Report, Italian Network of Earthquake Engineering University Laboratories.
- Paudel, Y., Botzen, W.J.W., Aerts, J.C.J.H. and Dijkstra, T.K. (2015), "Risk allocation in a public-private catastrophe insurance system: an actuarial analysis of deductibles, stop-loss, and premiums", *J. Flood Risk Manag.*, **8**(2), 116-134.
- ReLUIIS, ASSOBETON, CNI and DPC. (2012), Linee di indirizzo per interventi locali e globali su edifici industriali monopiano non progettati con criteri antisismici, Available online at [www.reluis.it](http://www.reluis.it).
- Rose, A. (2004), "Economic principles, issues, and research priorities in hazard loss estimation", *Model. Spatial Econom. Imp. Disasters*, Springer, 13-36.
- Savoia, M., Mazzotti, C., Buratti, N., Ferracuti, B., Bovo, M., Ligabue, V. and Vincenzi, L. (2012), "Damages and collapses in industrial precast buildings after the Emilia earthquake", *Ing. Sismica*, **29**(2-3), 120-130.
- Vamvatsikos, D. and Cornell, C.A. (2002), "Incremental dynamic analysis", *Earthq. Eng. Struct. Dyn.*, **31**(3), 491-514.
- Vanmarcke, E.H., Cornell, C.A., Gasparini, D.A. and Hou, S. (1976), *SIMQKE: A Program for Artificial Motion Generation*, Civil Engineering Department, Massachusetts Institute of Technology.
- Vanzi, I., Marano, G.C., Monti, G. and Nuti, C. (2015), "A synthetic formulation for the Italian seismic hazard and code implications for the seismic risk", *Soil Dyn. Earthq. Eng.*, **77**, 111-122.
- Yang, T.Y., Moehle, J., Stojadinovic, B. and Der Kiureghian, A. (2009), "Seismic performance evaluation of facilities: methodology and implementation", *J. Struct. Eng.*, **135**(10), 1146-1154.
- Zoubek, B., Isakovic, T., Fahjan, Y. and Fischinger, M. (2013), "Cyclic failure analysis of the beam-to-column dowel connections in precast industrial buildings", *Eng. Struct.*, **52**, 179-191.

CC